Pergamon

Journal of Structural Geology, Vol. 20, No. 9/10, pp. 1291 to 1304, 1998

0191-8141/98/$ - see front matter

PII: S0191-8141(98)00068-6

Litho-structural layering within the Archean Lac du Bonnet Batholith, at AECL's Underground Research Laboratory, Southeastern Manitoba

R. EVERITT

Atomic Energy of Canada Limited (AECL), Underground Research Laboratory (URL), Pinawa, Manitoba, Canada R0E 1L0, E-mail: everittr@aecl.ca

A. BROWN, R. EJECKAM, R. SIKORSKY

Atomic Energy of Canada Limited (AECL), Whiteshell Laboratories, Pinawa, Manitoba, Canada R0E 1L0

and

D. WOODCOCK

Atomic Energy of Canada Limited (AECL), Underground Research Laboratory (URL), Pinawa Manitoba, Canada R0E 1L0

(*Received* 26 *September* 1997; *accepted in revised form* 20 *April* 1998)

Abstract—The Lac du Bonnet Batholith (LDBB) is one of many late to post-tectonic granites in the western Superior Province which appear to be compositionally homogeneous and structurally simple on the surface. However, mapping in the 443 m deep access shaft at the Underground Research Laboratory (URL), borehole logs, and detailed surface mapping clearly demonstrate that decametre-scale layering is widespread in the LDBB. Individual layers or litho-structural domains are distinguished by the type and abundance of xenoliths and late residual or metasomatic segregations, by auto-intrusive contacts, and by variations in style and orientation of mesoscopic fabric. The litho-structural domains are inconspicuous at surface due to their low dip and the flat topography; however, detailed mapping in the central part of the URL has identified their surface expression as a series of broad and open domes and intervening saddles.

The litho-structural domains host three systems of auto-intrusive dykes, sills, and recrystallized zones whose abundance and mode of occurrence change with depth. Late magmatic granodioritic dykes are the predominant rock type below 300 m depth at the URL, but the swarm narrows rapidly up-dip, and at surface is represented only by narrow zones of alteration and ductile deformation. Late pegmatite–aplite dykes are pervasive across all rock types at surface, but are limited to the larger granodiorite dykes at 420 m depth at the URL. The distribution of inclusions, alteration and fractures in the LDBB suggest the present topographic surface is close to the original roof zone of the batholith.

INTRODUCTION

The Lac du Bonnet Batholith (LDBB) is one of many late to post-tectonic granites emplaced in the western Superior Province, towards the end of the 2760–2670 Ma Kenoran event (McCrank *et al.*, 1981; Davis *et al.*, 1986; Stone *et al.*, 1989). It is a relatively undifferentiated and partly foliated porphyritic granite–granodiorite consisting, like many other Archean batholiths, of broadly related but not sequentially fractionated intrusions (Cerny *et al.*, 1987). These batholiths, and the LDBB especially, are noted for their structural and compositional homogeneity over extensive surface areas (MacLeod, 1980; McCrank, 1985; Cerny *et al.*, 1987; Beakhouse, 1991), and have been described as such in the literature. The Lac du Bonnet Batholith was selected for investigations by Atomic Energy of Canada Limited (AECL) as part of a programme to assess the concept of nuclear waste disposal in plutonic rocks of the Canadian Shield (Whitaker, 1987). The geology of the batholith was defined through surface and airborne studies and by 130 boreholes, some reaching depths of 1100 m. The subsurface structure has been further characterized in detail through mapping of the shafts and galleries of AECL's Underground Research Laboratory (URL).

The excavations and boreholes at the URL site provide a unique cross-section 1100 m deep by ~1500 m long through an Archean batholith. The underground mapping and boreholes clearly indicate that what appears on surface to be a homogeneous Archean granite, is in fact coarsely layered with vertical gradations in alteration, lithology and structure. The section also shows low-dipping thrust faults and associated splays, and subvertical intrablock fractures between the major faults. This paper describes the batholith structure as seen in this vertical section. A summary and interpretation of the faults and fractures at this site can be found in Everitt and Brown (1995), and in

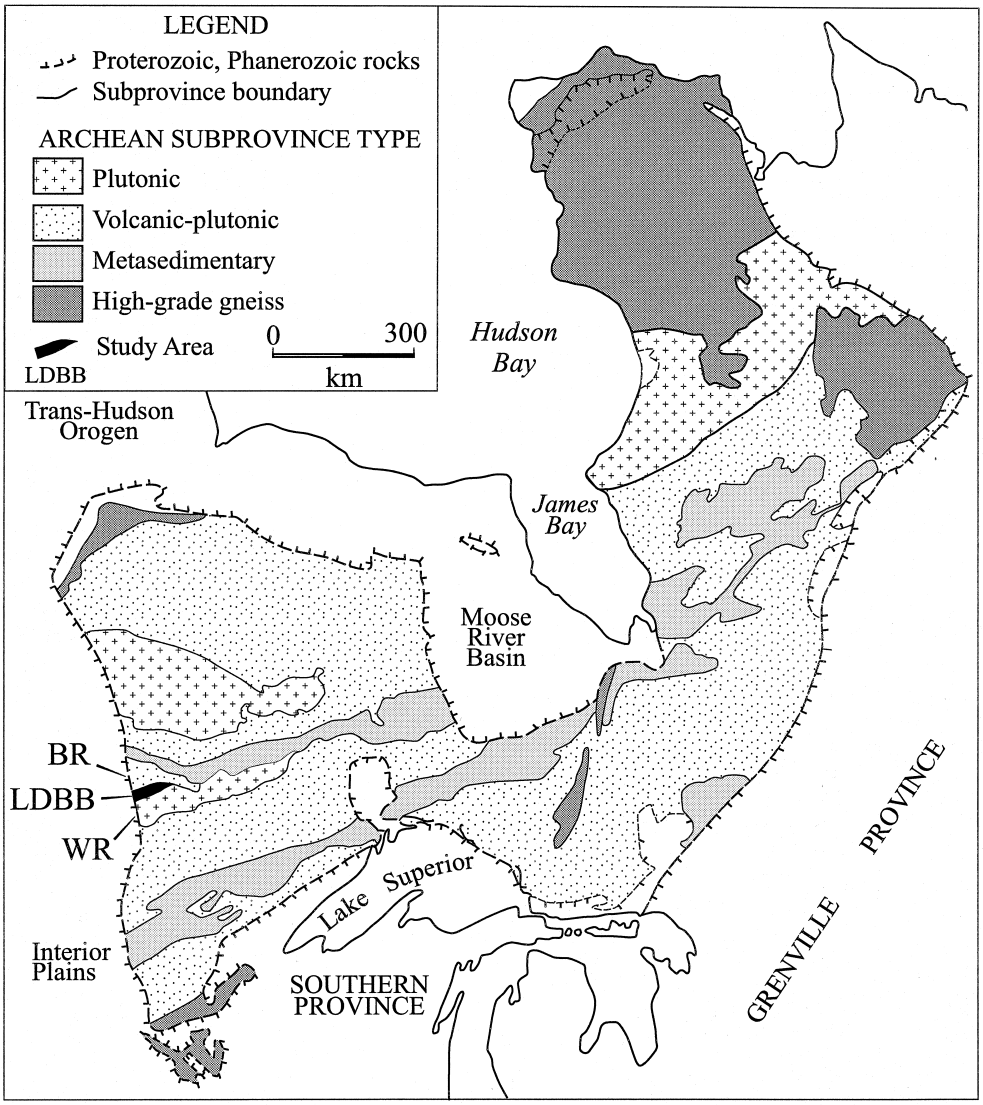

Fig. 1. Regional setting of the Lac Du Bonnet Batholith (LDBB). Modified from Card and Ciesielski (1986). BR—Bird River Subprovince. WR—Winnipeg River Subprovince.

Everitt *et al.* (1996). Orientations stated in the text are expressed as dip and dip direction (e.g. 25°/235°).

REGIONAL SETTING AND GENERAL GEOLOGY

The Lac du Bonnet Batholith is located on the western margin of the Superior Province (Figs 1 & 2). Its age has been investigated using a variety of methods (Krogh *et al.*, 1976; Cerny *et al.*, 1987; Kamineni *et al.*, 1990a, b); estimates for its crystallization age range from 2665 ± 20 Ma (U–Pb zircon) to 2568 ± 23 Ma (Rb/Sr whole-rock, Cerny *et al.*, 1987). The north contact of the batholith is sharp against a narrow belt of metavolcanic rocks in the Bird River Greenstone Belt. Its south contact is gradational against gneisses and migmatites of the Winnipeg River Subprovince (Beakhouse, 1977). West of the Winnipeg River, the batholith is largely covered by glacio-lacustrine sediments and by Palaeozoic carbonates, but its subcrop can be traced 20 km further to the west using aeromagnetic data.

Several authors have attempted to determine the subsurface extent and geometry of the LDBB (Beakhouse, 1977; Brisbin, 1979; MacLeod, 1980; Cerny *et al.*, 1987; Brown *et al.*, 1989). Tomsons *et al.* (1995) modelled the shape of the LDBB using gravity and magnetic data (Fig. 3). The north and south contacts dip steeply to the south, but shallow sill-like extensions exist on both the north and west sides. A 65° dip (Fig. 3) (Tomsons *et al.*, 1995) for the southern contact is consistent with mapping by Cerny *et al.* (1987) and Stone *et al.* (1989), and with borehole intersections (Ejeckam *et al.*, 1988). The shallower 50° dip interpreted from borehole intersections (Ejeckam *et al.*, 1988) may be due to fault repetition, and to a gradational interlayering of granite and tonalitic gneiss

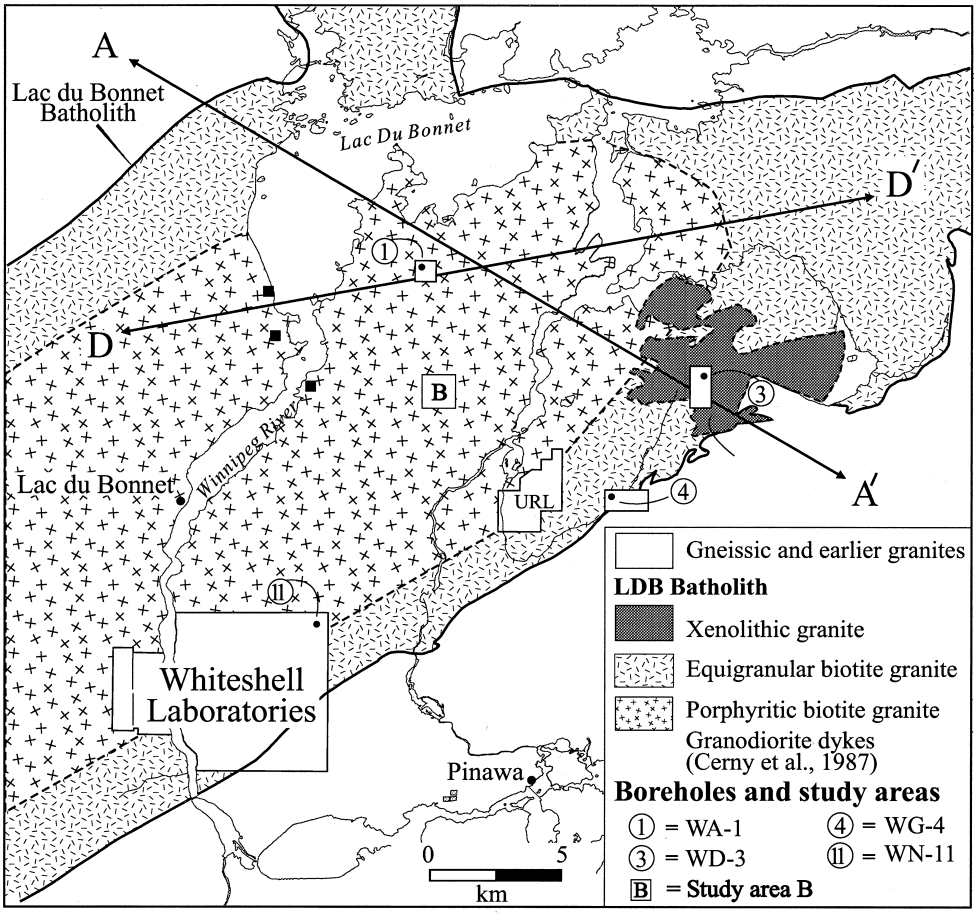

Fig. 2. Lac Du Bonnet Batholith (LDBB). General geology and sites referred to in text. URL—Underground Research Laboratory. 1, 3, 4, and study area B.—Surface borehole locations mentioned in text.

(Cerny *et al.*, 1987, Brown *et al.*, 1989). A gravity high recognized near the centre of the batholith (Brisbin, 1979; MacLeod, 1980), has been attributed to a near-surface xenolithic mass.

The batholith's maximum length, width and area are 85 km, 25 km, and 1800 km^2, respectively (McRitchie, 1971; McCrank, 1985; Stone *et al.*, 1989). Estimates of batholith volume range from 9060 to 45,000 km^3, depending on the interpretation of the batholith's shape.

Rock units

On the basis of mineralogy, texture, intrusive relationships, and geochemistry seen from surface ex-

Table 1. Comparison of rock units from surface and subsurface mapping of the Lac du Bonnet Batholith

	Rock units from surface mapping		Relative abundance
Rock units from subsurface (URL)	Cerny *et al.* (1987)	McCrank (1985); Stone *et al.* (1989)	surface, subsurface (URL)
xenoliths	1,2,3. predominantly tonalites and amphibolites but also some granitoids	same	10%? 15% but decreasing with depth
main phase	4. biotite granite	biotite granite, and textural variants.	80%? 40% but increasing with depth
auto-intrusive dykes, sills, and masses			
early group	not mentioned	irregular pegmatitic masses and porphyroblastic schlieren	~5%? 25%
middle group	5. late-tectonic biotite granodiorite dykes	not mentioned	trace 0–25%, increasing with depth
late group	6. pegmatite dykes	pegmatite–aplite dykes, and quartz veins	trace trace uniform distribution at surface but confined to granodiorite dykes below ~300 m

Note: Cerny's units 1–3 are not included in this comparison. They are confined to the eastern tip of the LDBB, and are considered by Stone *et al.* (1989) and McCrank (1985) to pre-date the LDBB.

Note: Relative abundances for surface from Stone *et al.* (1989) (recalculated to exclude xenolithic and early phases not found in URL). Relative abundances for subsurface based on subsurface mapping of URL (this paper)

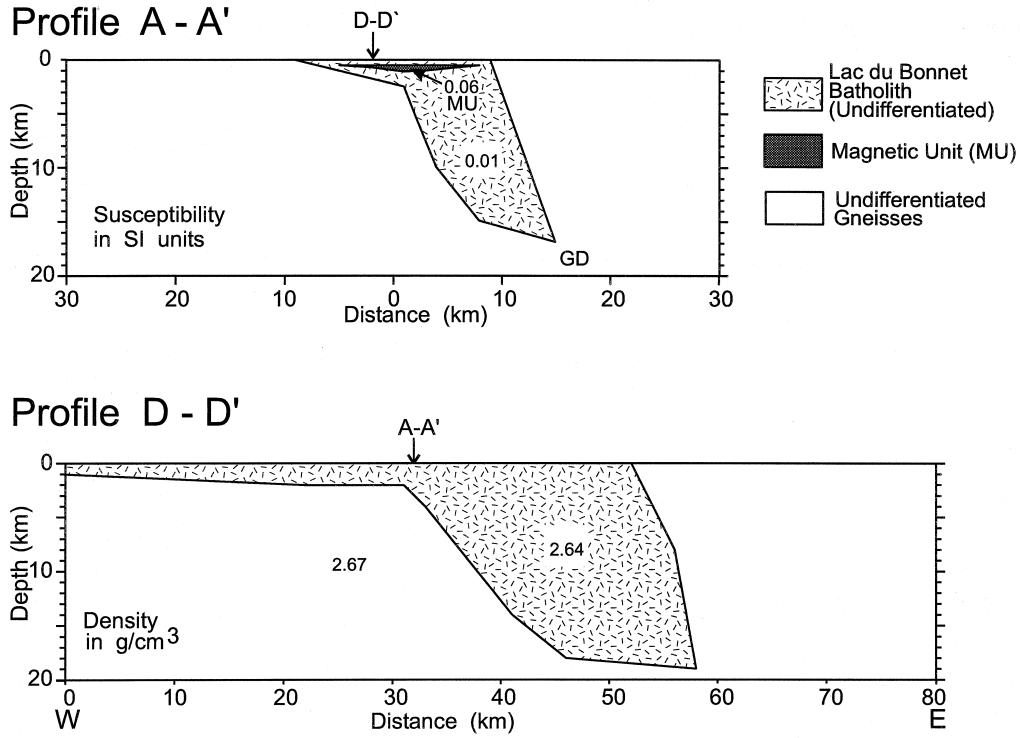

Fig. 3. Profiles across the Lac Du Bonnet Batholith. Modified from Tomsons *et al.* (1995). Northwest–southeast profile (A–A′), and east–west profile (D–D′). The four subdivisions of the LDBB shown in Fig. 2, and the older gneissic and other rocks around the LDBB are not differentiated in these sections.

posures, various authors have identified up to five rock units, with additional textural variants (Table 1). These may be broadly grouped as follows: metavolcanic xenoliths and earlier granites, the main phase of the LDBB granite, and several sets of consanguineous dykes.

The oldest granitic rocks within the LDBB (units 1, 2 and 3 of Cerny *et al.*, 1987, Table 1) are limited to the extreme eastern tip of the batholith outside of the study area (Fig. 2). Metavolcanic xenoliths are sparse except for the area immediately adjacent to the eastern end of the LDBB's southern contact. The dominant rock unit in surface outcrop (up to 80%), is a porphyritic granite–granodiorite (referred to as the 'main phase granite' in this paper). Several textural and compositional variants have been distinguished and can be seen in a single outcrop (Brown *et al.*, 1989). Late residual dykes and segregations are widespread but are comparatively rare. Irregular pegmatitic masses and porphyroblastic schlieren are most common in xenolith-rich areas (McCrank, 1985; Cerny *et al.*, 1987). Dykes of biotite granodiorite were the youngest of the major rock units recognized by Cerny *et al.* (1987), but only three small exposures were cited, and it was either not encountered or not recognized as a major rock unit by McCrank (1985) or others. Aplite and pegmatite dykes are widespread but of limited extent.

Alteration

Rock units range from a uniform grey, to red or pink where altered. Most reddening is associated with fractures, where the rock has been subject to long-term exposure to groundwater, and cuts across rock unit boundaries (Brown *et al.*, 1989; Stone *et al.*, 1989). Low-temperature alteration overprints the higher temperature forms of alteration around the major low-dipping fracture zones. Illite replaces epidote and biotite and Fe-oxides are removed, leaving the rock bleached in appearance.

Batholith structure

Drilling at several study areas (Fig. 2) shows that the structure of the LDBB is more lithologically varied and structurally complex than is apparent in outcrop. The surface drilling programme comprised over 130 boreholes for hydrogeological characterization. The boreholes are steeply plunging and reach depths greater than 1 km. These boreholes and surface mapping at many places throughout the batholith (D.C. Kamineni, A. Brown and others, unpublished data) demonstrate that folded coarse layering and several foliation fabrics are widespread in the main intrusive

phase of the batholith, but these results have not been compiled.

The present topographic surface of the batholith is thought to be close to the original roof zone of the intrusion. This interpretation was based on the distribution and orientation of xenolithic areas, and by the variation in degree and type of alteration within the upper 200 m of the batholith (Brown *et al.*, 1989).

The ENE-trending batholith is divided longitudinally into a shallow northern tongue and a steeply (65–70°) S-dipping portion over 15 km deep (Fig. 3). Layers of xenolithic, schlieric and compositionally banded granite (up to tens of metres thick), are widespread and locally common to at least the investigated depth of 1100 m. Within this coarse layering, and roughly concordant with it, are smaller-scale compositional banding, and metre-scale lenses of coarse, leucocratic pegmatoidal segregations. The layering is folded into broad, open, elongated domal antiforms and synforms. Evidence of general stretching suggest that folding is due to differential advance during intrusion. Stretching lineations at the east end of the batholith plunge 65° NE. Small-scale doubly-plunging folds in the metre-scale banding parallel major folding in the layering and plunge an average of 25° both northeast and southeast.

Small-scale foliations include: parallelism of biotite, platy feldspar laths, feldspars and quartz lenses, compositionally differentiated lenses (2–10 cm long and under 1 cm thick), and 10–20 cm long quartzo-feldspathic lenses that parallel larger pegmatite dykes in several common orientations. These all have roughly consistent attributes over wide areas of the batholith (data on the general structure of the batholith will be the subject of a future paper).

The following examples provide a sampling of the internal structure as seen in boreholes along a NW–SE profile (profile A–A′, Fig. 3) across the batholith.

1. Batholith Footwall. Borehole WA1 (Fig. 2) is collared near the northern contact, where gravity modelling suggests the batholith thins to a tapering wedge. Homogeneous main phase granite predominates to a depth of 740 m, but this becomes schlieric, and then xenolithic near the end of the borehole (unfortunately, the borehole was not long enough to intersect and confirm the batholith contact).
2. Batholith Interior. Boreholes from the centre of the batholith (study area B in Fig. 2) intersect the longest intervals of homogeneous main phase granite; xenolithic or heterogeneous zones are sparse.
3. Batholith Roof Zone. Boreholes collared near the southern contact of the batholith (Areas 3, URL, and the Whiteshell Laboratories (Fig. 2)) show the greatest variety of rock types, and the most pronounced decametre-scale layering. Borehole WD3 contains large xenolithic zones; borehole WN11 contains large zones of main phase granite with swarms of granodiorite dykes; and both boreholes differ from borehole WG4 which comprises relatively homogeneous granite.

URL GEOLOGY

The URL (Fig. 4) includes a vertical (access) shaft that extends to a depth of 443 m and several hundred metres of tunnels at depths of 240 and 420 m from surface (the 240 and 420 levels, respectively). Additional exposure is provided by raise-bored ventilation shafts, a timber-framed raise at the 420 level, and small shaft stations in the main access shaft at depths of 130 m and 300 m. Boreholes from the base of the shaft and the deepest level provide an additional 600 m of vertical exposure.

The URL (access) shaft and the various tunnels at each of the four levels were mapped during excavation. Shaft mapping was done from a suspended staging used to install the shaft framing and utilities during sinking.

The shaft mapping results are shown in Fig. 5(a & b). The shaft has a rectangular cross-section to 257 m depth. The geology, as seen on each of its four walls, is shown in Fig. 5(a). The shaft between 257 m and 442 m depth has a circular cross-section, and the geology as seen on the unrolled surface of this cylinder is shown in Fig. 5(b). The numerals on the left side of each shaft segment are lithostructural domains (also shown in Fig. 6). Short descriptions of each lithostructural domain or other distinctive features are provided to the right side of each shaft segment.

Lithostructural domains

The geology as seen in the URL shaft (Fig. 5a & b) and from a deep pilot borehole from the base of the shaft (Fig. 6) is dominated by decametre-scale compositional layering. These layers or lithostructural domains are distinguished by the type and abundance of xenoliths and late residual or metasomatic segregations, by auto-intrusive contacts, and by variations in style and orientation of decimetre-scale fabric elements. Contacts range from sharp to gradational, and most domains can be traced at least 500 m from the shaft, through their intersections with the vent raises, the tunnels at each of the four levels, and the extensive borehole arrays surrounding the excavations. Individual domains average about 25 m thick, dip about 15–30° SE, and strike northeast. These domains are in turn cross-cut by granodiorite and pegmatite dykes as shown in Fig. 5(a & b).

The lithostructural domains are not conspicuous at the surface. This is due to a combination of factors including: the low topography, the thickness and low

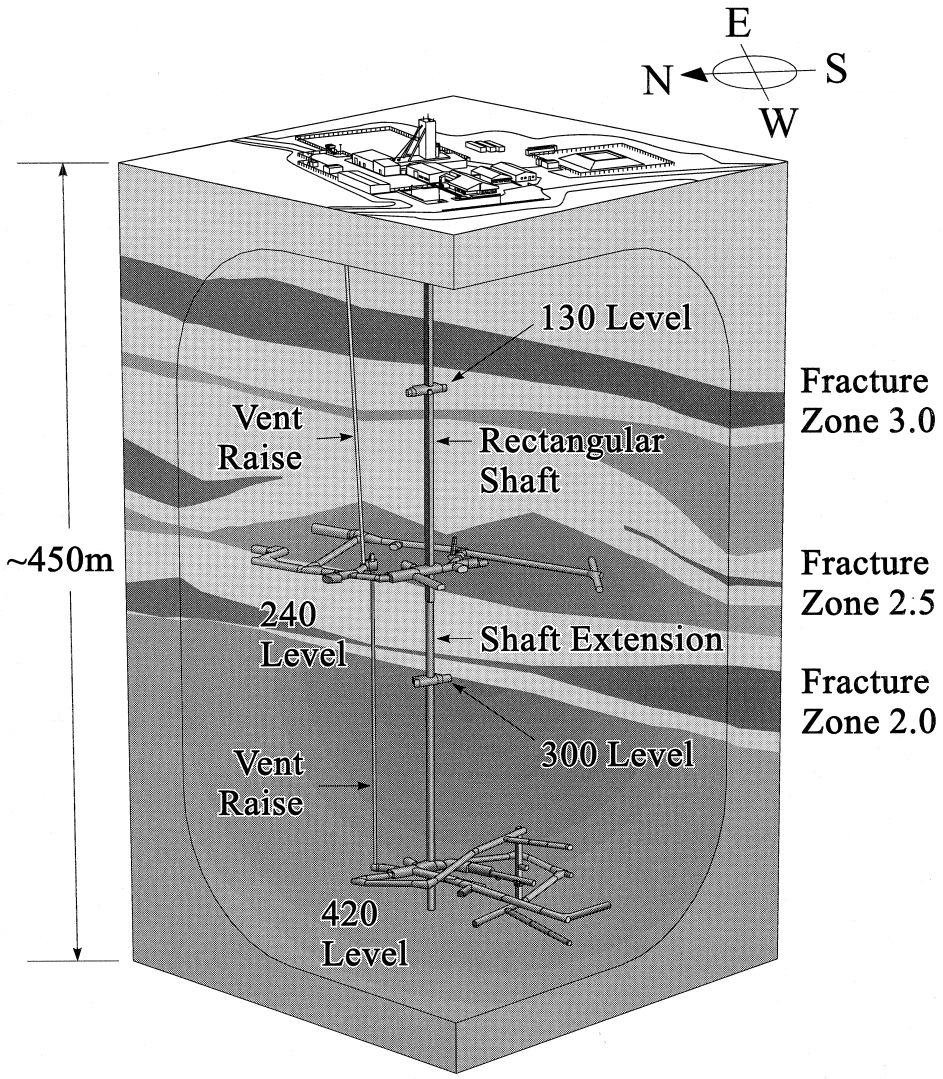

Fig. 4. Layout of the Underground Research Laboratory (URL) showing the excavations, the low-dipping thrust faults (dark grey), the alteration haloes associated with fractures (light grey), and unfractured and unaltered granite (medium grey).

dip angle of individual domains, and to variations in their composition, texture and structure along strike. However, detailed mapping in the central part of the URL (Stone *et al.*, 1989; Brown *et al.*, 1989) has identified their surface expression as a series of broad open domes and intervening saddles (Brown *et al.*, 1989, their figs 2 and 7).

A close-up of the contacts and fabric differences between three lithostructural domains intersected by the shaft is shown in Fig. 7. Here, an example of what on surface would be described as 'massive main phase granite' (Fig. 7, 142–160 m depth) separates two lithostructural domains of xenolithic granite. The xenoliths are composed of amphibolite from the invaded country rock. These are set in a coarse-grained to pegmatitic granite matrix that is strongly flow banded. The following features suggest differential movement and mingling of incompletely solidified components of the batholith roof zone, with the 'main phase granite' behaving more rigidly than the xenolithic granite at this location.

1. A fold in the flow banding of the upper xenolithic granite is abruptly truncated against the contact with the 'main phase granite' (Fig. 7, ~140–142 m depth).
2. Xenoliths, particularly those in the lower domain, are strongly flattened within 5 m of the contact, whereas xenoliths at a greater distance are undeformed. Undeformed xenoliths adjacent to the 'main phase granite' tend to have their long axes aligned parallel to the contact, but xenoliths further from the contact are more randomly oriented (Fig. 7, > 165 m depth).
3. Compositional layering in the 'main phase granite' within 5 m of the contact displays boudinage structure (Fig. 7, ~142 m depth).
4. A pegmatitic lens with very coarse microcline megacrysts is wedged against and is concordant with the lower contact of the 'main phase granite'. Some of

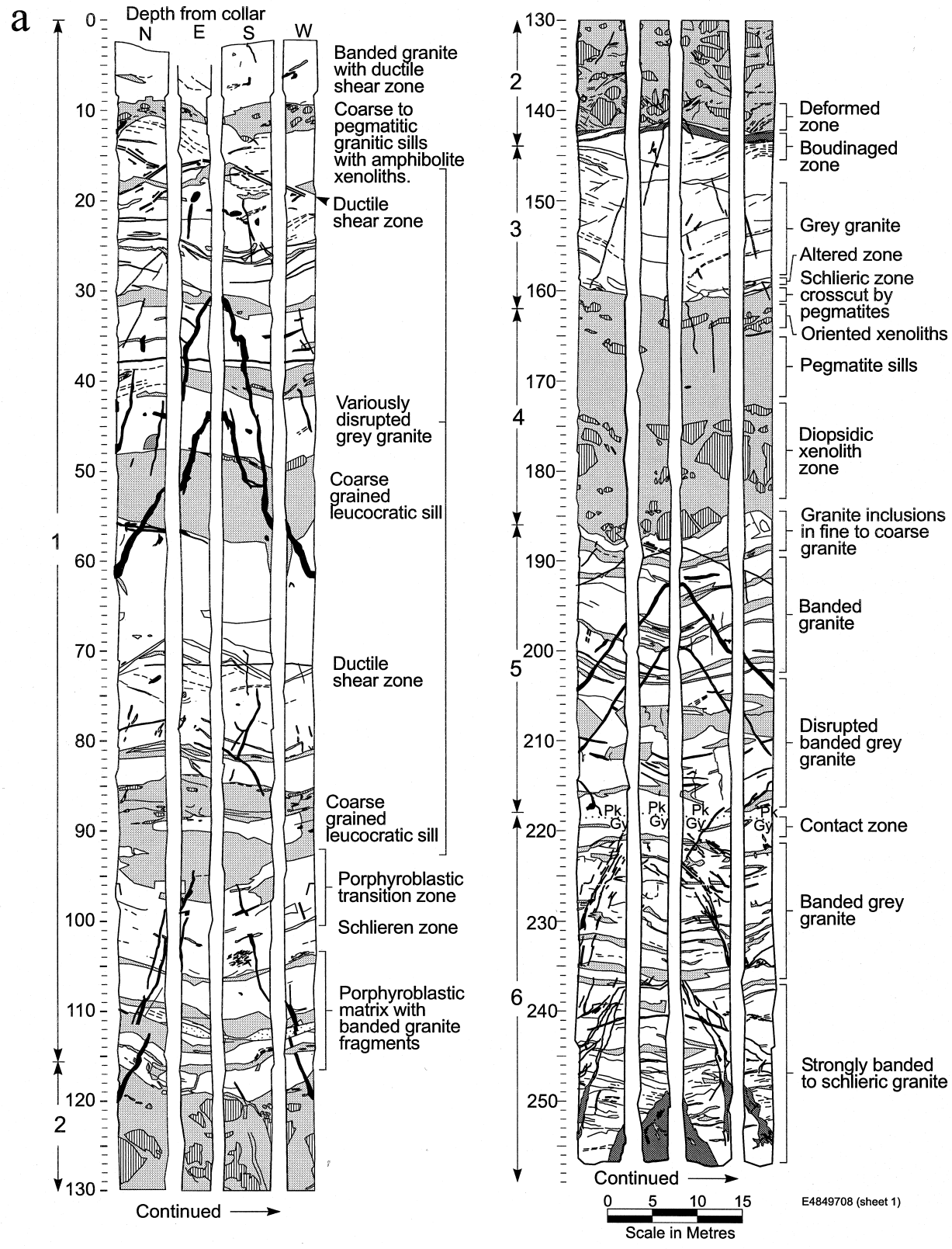
a
Depth from collar
N
E
S
W
Banded granite with ductile shear zone
Coarse to pegmatitic granitic sills with amphibolite xenoliths.
Ductile shear zone
Variously disrupted grey granite
Coarse grained leucocratic sill
Ductile shear zone
Coarse grained leucocratic sill
Porphyroblastic transition zone
Schlieren zone
Porphyroblastic matrix with banded granite fragments
Continued
Deformed zone
Boudinaged zone
Grey granite
Altered zone
Schlieric zone crosscut by pegmatites
Oriented xenoliths
Pegmatite sills
Diopsidic xenolith zone
Granite inclusions in fine to coarse granite
Banded granite
Disrupted banded grey granite
Contact zone
Banded grey granite
Strongly banded to schlieric granite
Pk Gy
Continued
0 5 10 15
Scale in Metres
E4849708 (sheet 1)

Fig. 5(a).

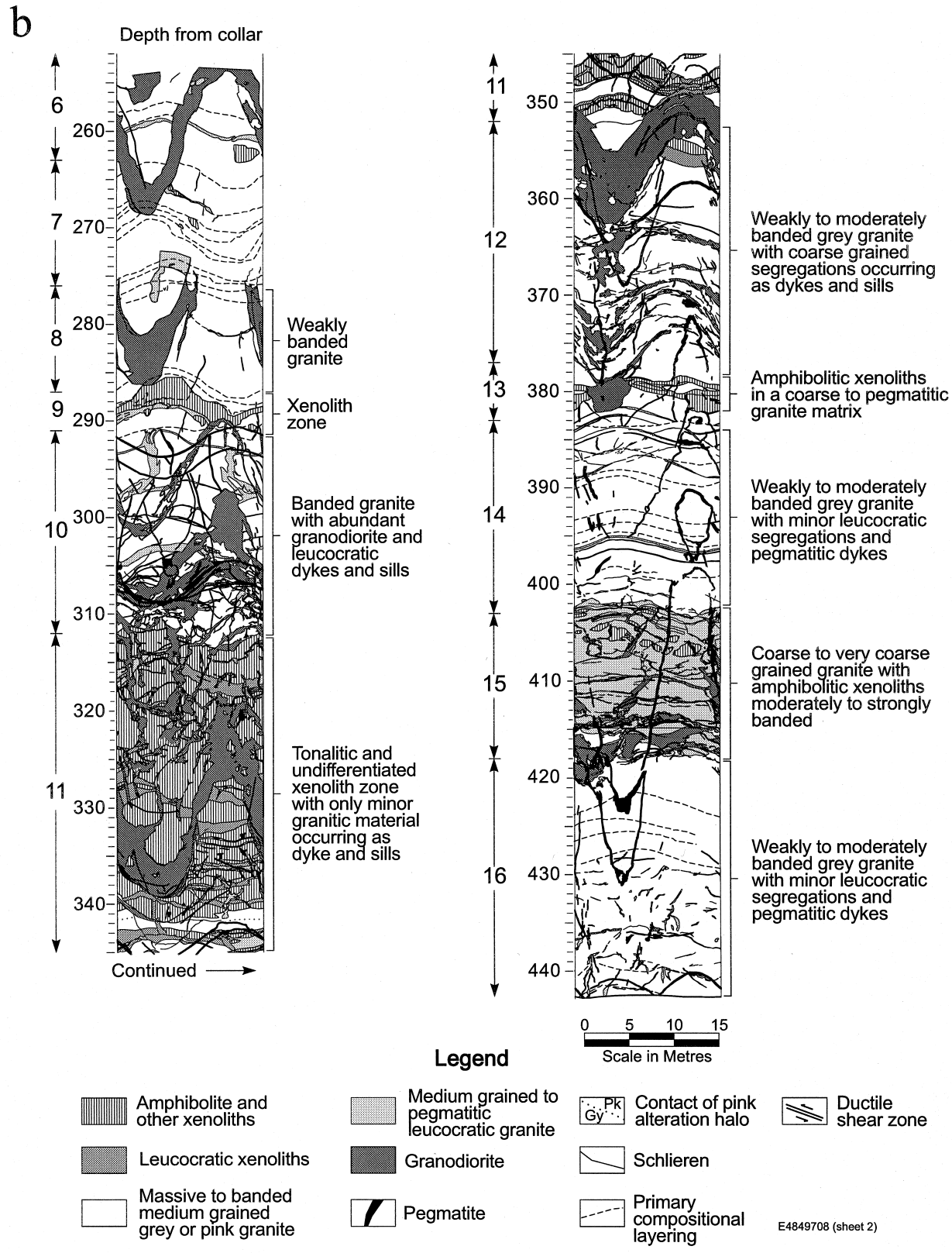

Fig. 5. Simplified geological map of the URL access shaft. The main phase of the granite is shown in white, while the metavolcanic xenoliths and three generations of later dykes, sills and masses are shown in the various shades of grey. The four walls of the rectangular portion of the shaft (0–257 m depth) is shown in (a). From left to right are shown the north, east, south, and west walls. The shaft between 257 m and 442 m has a circular cross-section as shown in (b). The numerals on the left side of each shaft segment are the lithostructural domain reference numbers (see also Fig. 6), and the depth (in metres) from the shaft collar. To the right side of each segment are short descriptions of the domains or of other distinctive features.

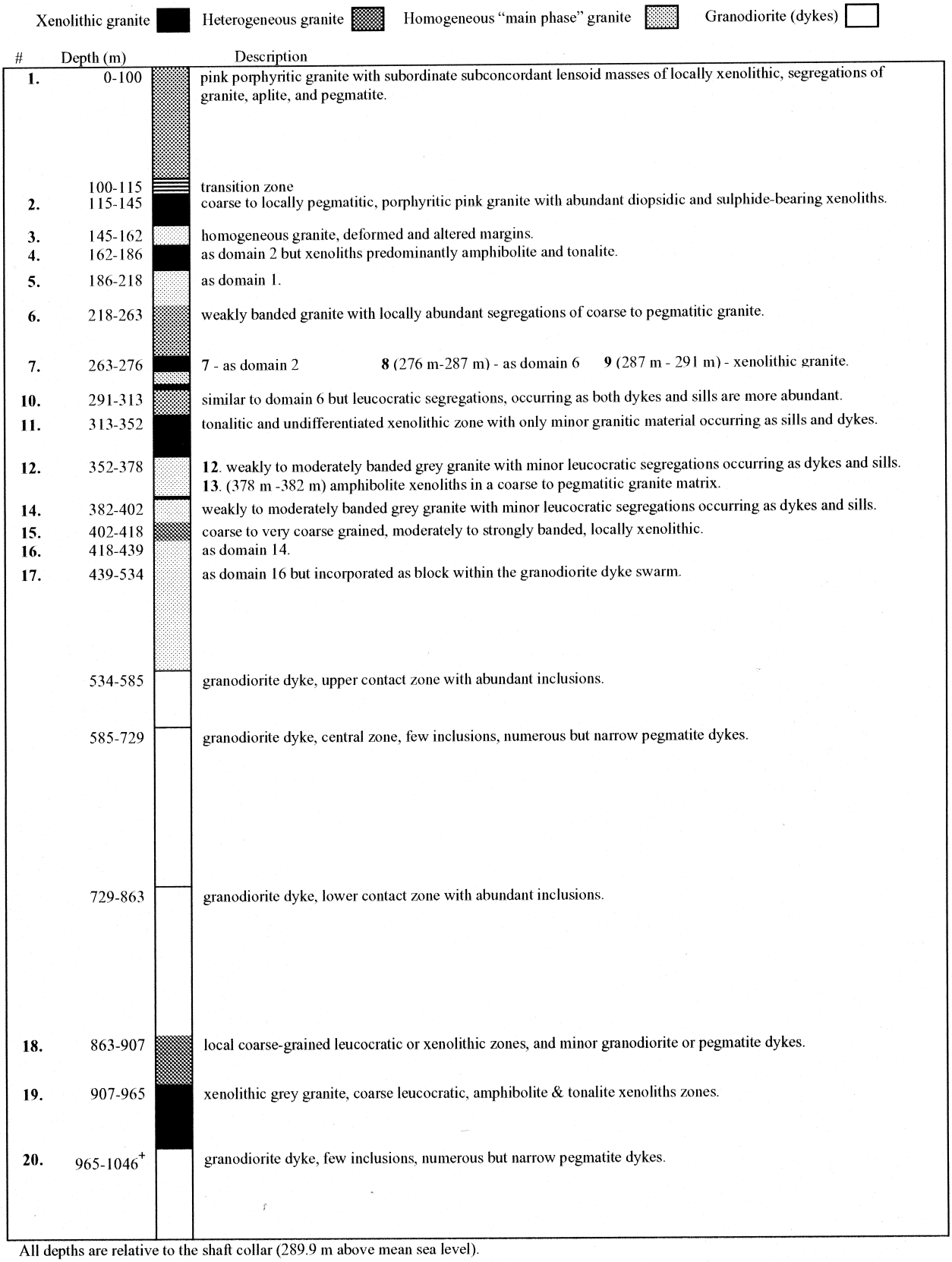

Fig. 6. Lithostructural domains in the URL access shafts (to 443 m depth) and in the deep stress measurement borehole (443–1046 m depth). The reference domain for each number is shown in the far left column, followed by the depth interval (as seen in the shaft to 445 m depth, and projected from the deep pilot borehole below this). A description of each lithostructural domain follows and includes a graphic log which illustrates the relative heterogeneity of the batholith with depth.

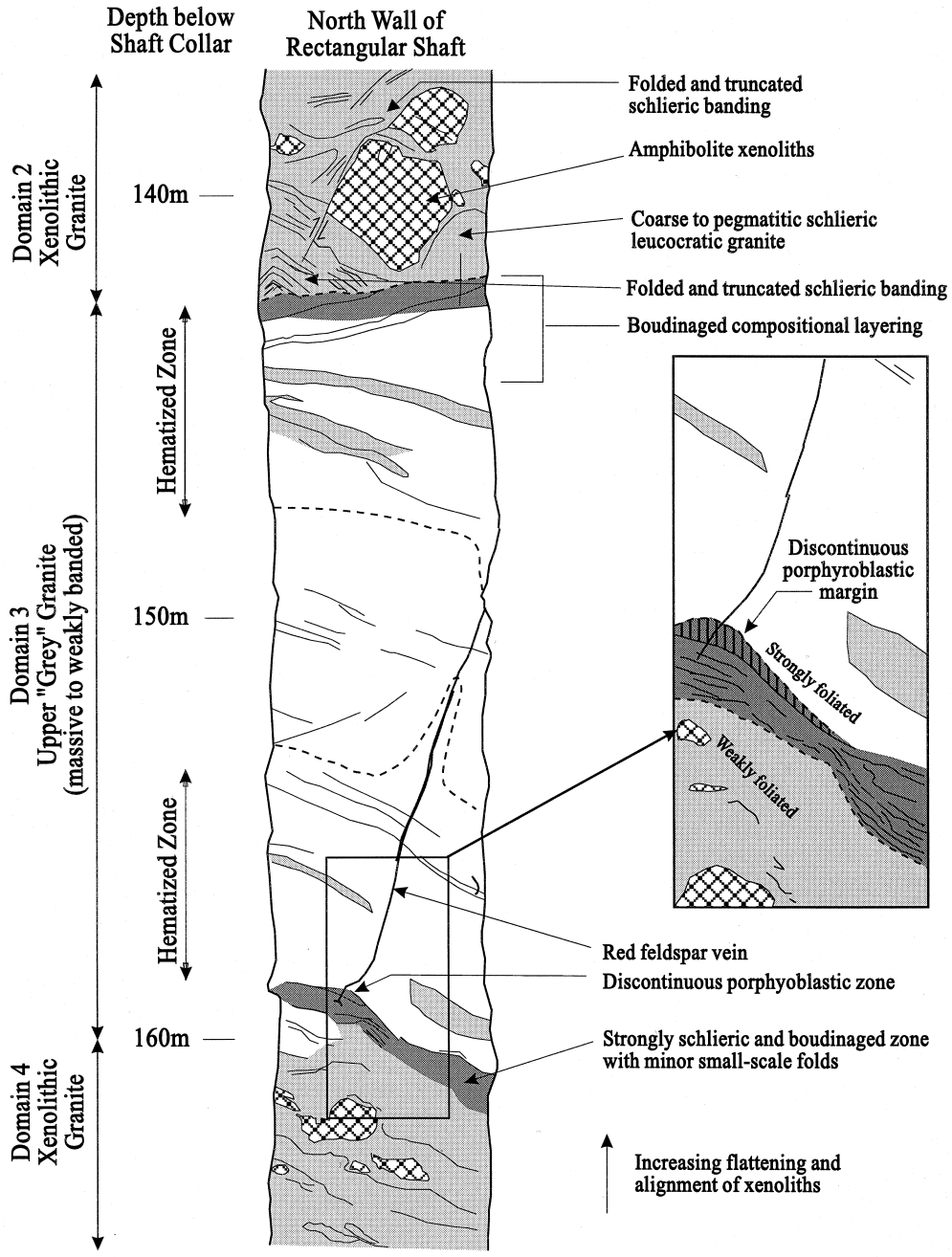

Fig. 7. Simplified geological map of three lithostructural domains exposed in the URL shaft. Area shown is an enlargement of the north wall of the rectangular shaft between 135 m and 165 m depth as shown in Fig. 5(a) preceding. The inset shows an enlargement of the contact at 160 m depth.

Table 2. Descriptive list of subsurface mapping units for the Lac du Bonnet Batholith

Rock Unit	Description
xenoliths	chiefly amphibolite, granodiorite and tonalite
main phase granite	chiefly medium grained granite or biotite granite; massive to schlieric, occurs as main mass of LDBB, and as rare auto-intrusive dykes.
auto-intrusive dykes, sills, and masses	
early group	leucocratic granite; irregular masses or sills, or less frequently as steeply-dipping dykes. medium to coarse or very coarse grained, and porphyritic to porphyroblastic.
middle group	granodiorite dykes
late group	chiefly pegmatite and pegmatite–aplite dykes, but also transitional with quartz–feldspar dykes or masses, and quartz-epidote–chlorite veins or fracture fillings.

Note: for convenience, the underlined names are used to refer to these units in the text

this material has been injected into a fracture which intrudes several metres into the 'main phase granite' (Fig. 7, ~160 m depth, and inset).

5. The matrix granite in the xenolithic domains is coarse grained to pegmatitic, megacrystic, and intensely reddened. This reddening crosses domain boundaries, and affects the periphery of the 'main phase granite' (Fig. 7, ~142–148 m and 154–160 m depth).

Drilling from the 130 level Shaft Station has shown that the mass of 'main phase granite' in this example thins rapidly and terminates 20 m both up-dip, and within a similar distance to the southwest along strike. This evidence of limited extent, together with the relative age relationships listed above suggest that this specific mass is a large inclusion, rather than a sill of the 'main phase granite'.

Rock units

The metre-scale rock units that, in varying combinations, comprise the lithostructural domains are largely equivalent to those defined from surface mapping (Tables 1 & 2). However, their relative abundances are substantially different from those seen at surface, and their relationships are more clearly defined. Continuous vertical exposures have also shown that composition and texture are not constant for a single rock unit, but vary along strike and down dip. This is shown to the greatest extent by the granodiorite dykes.

Main phase granite. The unshaded areas in Fig. 5 are the main phase granite of the batholith (Tables 1 & 2), and its description matches that of McCrank (1985) and Cerny *et al.* (1987) from surface mapping. In the subsurface, its fabric ranges from massive to schlieric, its texture from equigranular to porphyritic (Fig. 8a). Xenolithic horizons (Fig. 8b) are common to depths of 1 km, but these diminish in size and frequency with depth. Metre- and larger-scale layering shows a consistent orientation in the URL with a mean value of 22°/122° (Fig. 9a). The lithostructural domain boundaries and the small-scale gneissic layering are thought to represent primary compositional layering in the batholith. This rock unit is host to the three systems of consanguineous dykes, sills, and recrystallized zones which follow.

Leucocratic granite. This unit comprises a heterogeneous assemblage of residual leucocratic segregations and porphyroblastic zones. Textures range from aplitic to pegmatitic, and porphyritic to equigranular. The contacts of this unit range from sharp to gradational, and are generally parallel to the layering of the main phase granite. The largest zones (up to 30 m thick) occur in association with xenolithic horizons, and have complex margins and internal fabrics. In the upper 150 m of the shaft, two sets of fine-grained dykes intrude porphyritic granite, but individual dykes merge downwards into the granite they intrude at higher elevation. The dykes have strikes at approximately 145° and have opposing 45° dips, and normal offset of the layering of the host granites, indicating the general extension along the long axis of the batholith.

Granodiorite dykes. At surface, this rock unit is represented by very minor outcrops of dyke material observed outside the URL site by Cerny *et al.* (1987) and, at the URL site, by narrow zones of epidote-filled fractures, haematization, and cataclasite in the host granite. This is in marked contrast to its occurrence in the subsurface at the URL, where it is well exposed by numerous intersections with boreholes and excavations. This rock unit occurs as a dyke swarm which increases in both size and complexity with depth (Figs 5, 6 & 8). Initial petrographic analyses of samples from the 240 level confirmed Cerny *et al.*'s, granodiorite classification for this unit, but subsequent analysis of additional samples from the 420 level indicate this unit straddles the granite–granodiorite boundary of the IUGS classification, with substantial overlap into the (biotite) granite field (IUGS, 1973).

At the 240 level, these dykes comprise up to 10% of the rockmass, and are up to 5 m thick with well-developed chilled margins and flow banding (e.g. Fig. 8c). Flow banding is defined by a preferred alignment of biotite crystals, biotitic aggregates and inclusion trains. At the 300 and 420 levels of the URL, granodiorite occurs as a stockwork of large dykes and minor interconnecting sills (Fig. 8d), and is the most abundant rock type. The largest dykes at and below the 420 level are massive and medium grained and, apart from the orientation of the foliation, are indistinguishable in hand specimen from the biotite granite they intrude.

Between the surface and the 420 m depth, the granodiorite dyke swarm is represented by a small number of very large discordant dykes with an average orientation of 63°/235° (dyke dip length > 1000 m, and dyke thickness up to 15 m). The shallow-dipping set shown in Fig. 9(b) (22°/196°) is limited to the area below ~300 m depth, where it represents fissure fillings formed by disintegration of the granite slabs between the steeply-dipping dykes.

The dykes were intruded along ductile normal faults (most evident above 240 m depth). These are marked by the development of drag folds and local foliations, and by boudinage developed in both the adjacent host rock and in quartz veins present in the extreme 'tip regions' of the swarm.

As with the earlier granite dykes described in the preceding section, the orientation and normal sense of offset associated with this swarm indicate a general extension parallel to the long axis of the batholith, during intrusion of the granodiorite.

Pegmatite dykes. This group includes pegmatite and aplite dykes, quartz veins and irregular quartzo-feldspathic masses. At surface and at the 240 level, both quartz veins and the major and minor pegmatite dykes

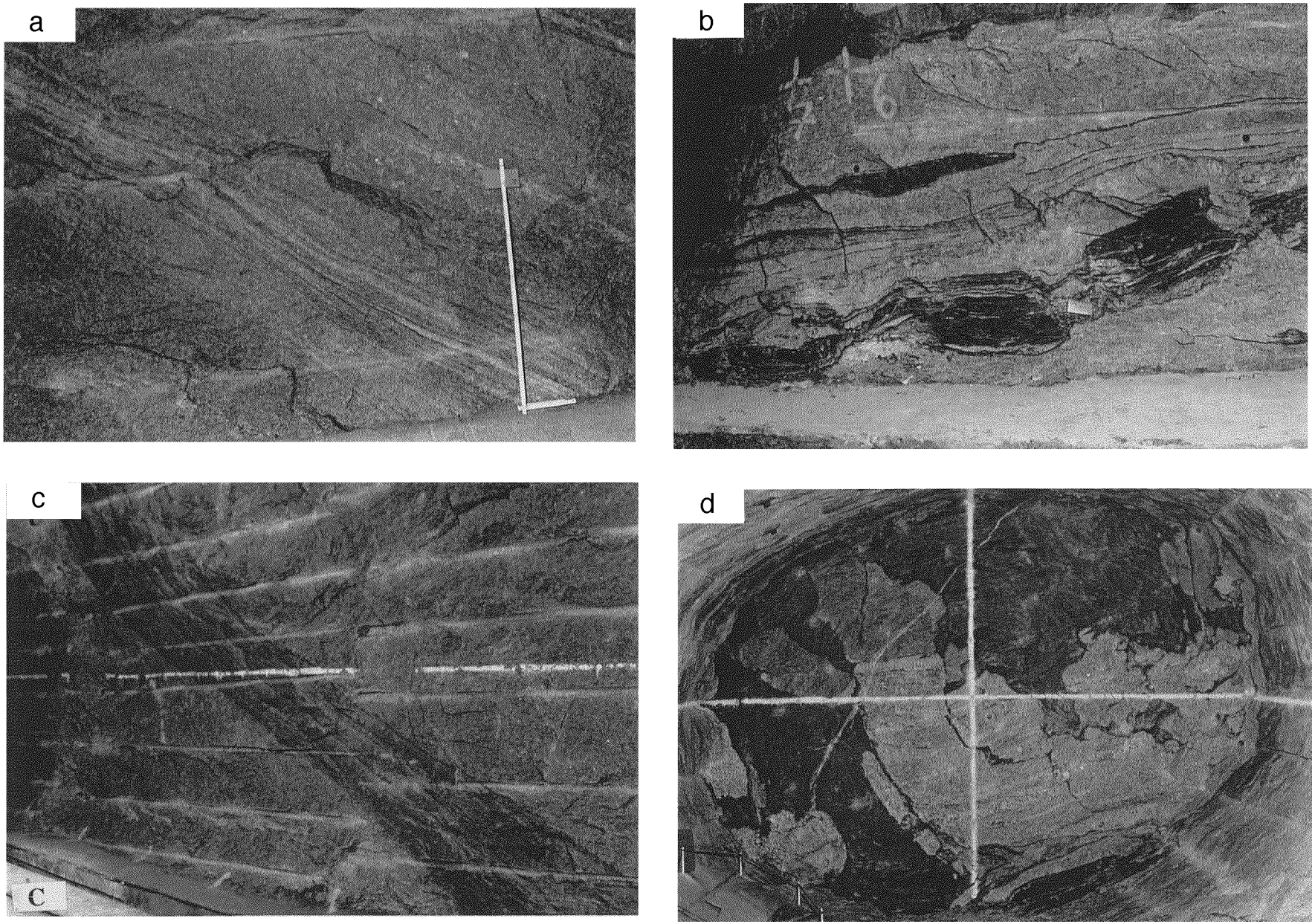

Fig. 8. Rock units and structures recognized at depth in the URL. (a) Compositional layering in the main phase granite as seen on a tunnel wall at the 420 level. Height of ruler is 80 cm. (b) Boudinage structure and layering in xenolithic granite as seen in a tunnel wall at the 420 level. The individual boudins are approximately 0.5 m by 0.25 m. (c) Typical exposure of a granodiorite dyke as seen in a tunnel wall at the 240 level. The dyke (dark grey) runs diagonal from upper left to lower right. Flow banding is pervasive throughout the dyke and is parallel to the dyke walls. The dyke cross-cuts the main phase granite. The white line is 1.2 m from the tunnel floor. (d) Inclusions within the interior of a large granodiorite dyke (dark grey) as seen in the vertical wall of a tunnel face at the 420 level. The tunnel face is approximately 2.5 m by 3.5 m. The dyke is approximately 15 m thick; its walls are nearly perpendicular to the tunnel axis and are not visible in this view. The remnants of a lithostructural domain boundary are preserved within the inclusion to the centre left. Within the inclusion, the granite appearing medium grey is part of the main phase granite, while the underlying light grey rock is part of a leucocratic granite sill.

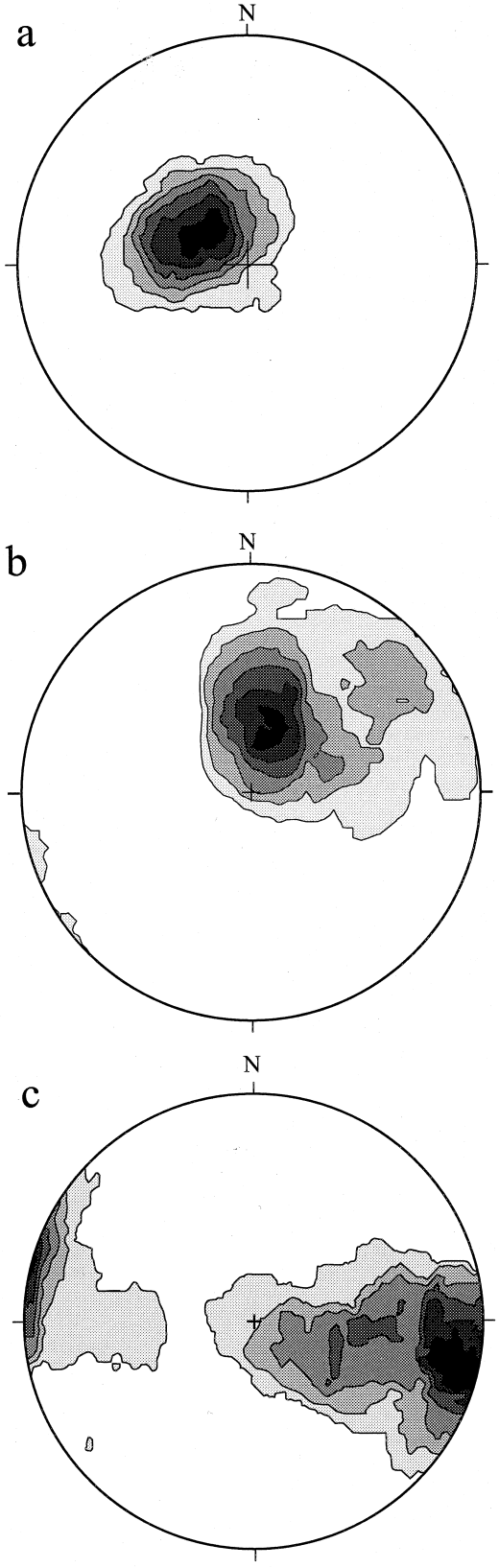

Fig. 9. Summary of structure orientations as seen in the URL excavations. Lower-hemisphere equal-area plot of poles contoured by the Schmidt method. (a) Large-scale compositional layering (93 poles, contour interval—3.5, 19, 38, 47.5, 57 and 66.5% per unit area). (b) Granodiorite dyke contacts (74 poles, contour interval—4.5, 9, 18, 22.5, 27, and 31.5% per unit area). (c) Late pegmatite dyke contacts (35 poles, contour interval—8, 9, 13.5, 22.5, 27, and 31.5% per unit area).

are pervasive across the whole map area with little if any clustering related to local rock type. At the 420 level, however, this group is confined to the larger granodiorite dykes. Their preferred orientations are summarized in Fig. 9(c). The poles plot along great circles but several sets are recognized; a dominant subvertical set (77°/283°), and an intermediate-dipping set whose orientation is partly controlled by the layering in the granodiorite.

Significance of structure at the URL. The vertical section provided by the URL shaft (Fig. 5a & b) and the borehole from the base of the shaft (Fig. 6) clearly show that the LDBB, rather than being simple and homogeneous, is in fact strongly layered and crossed by consanguineous dyke swarms. Most of this structure is not visible at surface due to the low dip of the layering, and to the rapid thinning of the various dyke swarms as they approach the present topographic surface. The low-dipping layering is interpreted as the result of: (1) primary magmatic to sub-magmatic flow producing mineral alignment and segregation into metre- to centimetre-scale layering, (2) inherited layering from the host rock (the xenolithic horizons), and (3) the intrusion of subconcordant sills and hydrothermal segregations, the latter producing the porphyroblastic horizons. The strongly layered and heterogeneous interval between the present topographic surface and approximately 550 m depth is tentatively interpreted as approximating the roof zone of the batholith. This is host to at least three generations of dykes. In the upper 150 m of the shaft, dykes associated with the leucocratic granite intrude porphyritic main phase granite, but individual dykes merge downwards into the granite they intrude at higher elevation. Similarly, the granodiorite dykes appear to merge with the biotite granites at depth, and their preponderance in the section below 400 m indicates that this unit may be more representative of the batholith interior. The orientation and normal offset associated with each dyke generation suggests at least local extension of the batholith in a direction parallel to the long axis of the batholith.

The data presented suggest batholith emplacement as a succession of magma pulses into this crystalline but still (locally) semi-ductile roof zone. A general extension of this roof zone is indicated by widespread two dimensional boudinage of layers, and the various dykes and sills described. The overall emplacement mechanism of the LDBB is not yet well understood. However, it may be similar to that described in Cruden and Launeau (1994) for the Lebel Stock, but in this case involving northward spreading of magma sheets from the ENE–WSW-trending boundary between the Winnipeg River Subprovince and the Bird River Greenstone Belt. This is consistent with the shape of the batholith as seen in section (Fig. 3a & b), with a sharp but shallow-dipping northern contact against the metavolcanic rocks of the Bird River

Greenstone Belt, and its steeper and gradational southern contact against the gneisses and migmatites of the Winnipeg River Subprovince.

SUMMARY AND CONCLUSIONS

The LDBB is a typical late-tectonic Archean batholith of the western Superior Province. It appears on surface to be homogenous and of simple structure, and has been described as such in the literature. The drilling results and excavation mapping at the URL, however, provide a vertical section that contradicts this view and attributes the apparently simple structure to a directional sampling bias. The LDBB is in fact characterized by coarse layering with a low to subhorizontal dip. It contains several sets of auto-intrusive dykes whose pattern and frequency are depth-dependent. The layering is obscured at surface by the low topographic relief, the low dip of the layering, the thickness of individual domains, and by changes in the composition and texture of individual domains along strike and down dip. However, detailed mapping at surface within a section of the URL site has identified their surface expression as a series of broad open domes.

The LDBB is similar in age, composition, and tectonic setting to many other felsic intrusions in the western Superior Province (not just the Winnipeg River Subprovince) and, by analogy with the present study, these other intrusions are probably more lithologically and structurally complex than was previously thought.

Acknowledgements—We would like to thank Alexander (Sandy) Cruden, Denver Stone, and Phil Simony for their constructive comments and advice in preparing this paper. We also thank Paul Gann, Gig Hiltz, Ed Jacobs and Fred Bilsky for their assistance in drafting the figures. The work was funded jointly by AECL and Ontario Hydro under the auspices of the CANDU Owners Group (COG). Copies of reports published by AECL are available from the Scientific Document Distribution Office, Atomic Energy of Canada Limited, Chalk River, Ontario K0J 1J0 Canada.

REFERENCES

Beakhouse, G. P. (1977) A subdivision of the western English River Subprovince. *Canadian Journal of Earth Sciences* **14,** 1481–1489.

Beakhouse, G. P. (1991) Winnipeg River Subprovince. In *Geology of Ontario*, eds P. C. Thurston, H. R. Williams, R. H. Sutcliffe and G. M. Stott, pp. 279–302. Ontario Geological Survey Special Volume 4, Part 1.

Brisbin, W. C. (1979) A gravity profile across the Lac du Bonnet batholith in southeastern Manitoba Atomic Energy of Canada Limited, Technical Record TR-17.

Brown, A., Soonawala, N. M., Everitt, R. A. and Kamineni, D. C. (1989) Geology and geophysics of the Underground Research Laboratory site, Lac du Bonnet Batholith, Manitoba. *Canadian Journal of Earth Sciences* **26,** 404–425.

Card, K. D. and Ciesielski, A. (1986) *DNAG ♯1. Subdivisions of the Superior Province of the Canadian Shield Geoscience Canada* **13,** 5–13.

Cerny, P., Fryer, B. J., Longstaffe, F. W. and Tammemagi, H. Y. (1987) The Archean Lac du Bonnet batholith, Manitoba: Igneous history, metamorphic effects, and fluid overprinting. *Geochimica et Cosmochimica Acta* **51,** 421–438.

Cruden, A. R. and Launeau, P. (1994) Structure, magnetic fabric and emplacement of the Archean Lebel Stock, SW Abitibi Greenstone Belt. *Journal of Structural Geology* **16,** 667–691.

Davis, D. W., Corfu, F. and Krogh, T. E. (1986) High precision U–Pb geochronology and implications for the tectonic evolution of the Superior Province. In *Workshop on Tectonic Evolution of Greenstone Belts*. eds M. J. deWit and L. D. Ashwal. Lunar and Planetary Institute, Houston, TX, Technical Report 86-10, pp. 77–79.

Ejeckam, R. B., Kamineni, D. C., Stone, D. and Thivierge, R. H. (1988) *Surface and Subsurface Geology of Permit Area 'G' in the Lac du Bonnet Batholith, Manitoba*. Atomic Energy of Canada Limited Technical Record, TR-462.

Everitt, R. A. and Brown, A. (1995) Geological Mapping of AECL Research's Underground Research Laboratory. A cross section of thrust faults and associated fractures in the roof zone of an Archean batholith. In *Proceedings of Fractured and Jointed Rock Masses, International Society for Rock Mechanics*, eds L. R. Myer, N. G. W. Cook, R. E. Goodman and C-F. Tsang, pp. 3–12. Balkema, Lake Tahoe, California.

Everitt, R. A., McMurry, J., Brown, A. and Davison, C. C. (1996) Geology of the Lac du Bonnet batholith, inside and out: AECL's Underground Research Laboratory, Southeastern Manitoba. Field Trip Guidebook B5, Geological Association of Canada/ Mineralogical Association of Canada. Annual Meeting, Winnipeg, Manitoba, May 27–29.

IUGS (International Union of Geological Sciences) Subcommission on the Systematics of Igneous Rocks (1973) Plutonic rocks, classification, and nomenclature. *Geotimes* **18,** 26–30.

Kamineni, D. C., Brown, A., Peterman, Z. and Stone, D. (1990a) GRadiometric ages, cooling rates and deformation of two granitic plutons in the Superior Province, Canadian Shield. *Geological Society of America* (Abstracts with Program) **22,** A244.

Kamineni, D. C., Brown, A., Peterman, Z. and Stone, D. (1990b) Early Proterozoic deformation in the western Superior Province, Canadian Shield. *Geological Society of America Bulletin* **102,** 1623–1634.

Krogh, T. E., Davis, G. L., Ermanovics, I. and Harris, N. B. W. (1976) U–Pb isotopic ages of zircons from the Berens block and English River gneiss belt. *Proceedings of 1976 Geotraverse Conference, University of Toronto* **12-1,** 46.

MacLeod, I. N. (1980) A gravity survey of Lac du Bonnet Batholith research area RA-3, Lac du Bonnet, Manitoba. In *Applied Geoscience Branch, Whiteshell Laboratories, Pinawa, Manitoba*. Unpublished report.

McCrank, G. F. D. (1985) *A geological survey of the Lac du Bonnet Batholith, Manitoba*. Atomic Energy of Canada Limited, Report AECL-7816.

McCrank, G. F. D., Misiura, J. D. and Brown, P. A. (1981) *Plutonic Rocks in Ontario*. Geological Survey of Canada, Paper **80-23**.

McRitchie, W. D. (1971) The petrology and environment of the acidic plutonic rocks of the Wanipigow–Winnipeg Rivers region, southeastern Manitoba. In *Geology and geophysics of the Rice Lake region, southeastern Manitoba (Project Pioneer)*, eds W. D. McRitchie and W. Weber, Vol. 71-1. Manitoba Mines Branch, Publication.

Stone, D., Kamineni, D. C., Brown, A. and Everitt, R. (1989) A comparison of fracture styles in two granite bodies of the Superior Province, *Canadian Journal of Earth Sciences*. **21,** 387–403.

Tomsons, D. K., Lodha, G. S., Street, P. J. and Auger, J. L. F. (1995) *A Bouguer gravity anomaly map and geophysical interpretation of the geometry of the Lac du Bonnet Batholith*. Whiteshell Research Area, Southeastern Manitoba Atomic Energy of Canada Limited, Technical Record, TR-633, COG-94-096.

Whitaker, S. H. (1987) Geoscience research for the Canadian Nuclear Fuel Waste Management Program. *Radioactive Waste Management and the Nuclear Fuel Cycle* **8,** 145–196.